EPJ Web of Conferences **40**, 11004 (2013)
DOI: 10.1051/epjconf/20134011004

Magnetostriction of permalloy epitaxial and polycrystalline thin films

Taiki Ohtani, Tetsuroh Kawai, Mitsuru Ohtake, and Masaaki Futamoto

Faculty of Science and Engineering, Chuo University, 1-13-27 Kasuga, Bunkyo-ku, Tokyo 112-8551, Japan

Abstract. Permalloy epitaxial films of (111), (100), and (110) orientations and a polycrystalline thin film are prepared. Sinusoidal waveforms of magnetostriction are observed when the polycrystalline and the (111)-oriented epitaxial films are measured under rotating magnetic fields ranging from 10 to 1000 Oe. On the contrary, the (100)- and the (110)-oriented films, respectively, show a triangle waveform and a waveform consisting of a mixture of triangular and sinusoidal shapes under low magnetic fields. The waveform variation is interpreted by considering the magnetization structure of magnetically unsaturated film with an in-plane magnetic symmetry related with the crystallographic orientation. The waveforms deformed from sinusoidal shape vary to sinusoidal with increasing the magnetic field. Magnetically saturated (100)- and (110)-oriented films show sinusoidal waveforms. The saturated magnetostriction values are determined as $\lambda_s = 5 \times 10^{-6}$, 4×10^{-6}, 3×10^{-6}, and 6×10^{-6} for the (111), the (100), the (110) epitaxial and the polycrystalline films, respectively.

1 Introduction

Permalloy (Py: Ni - 20 at. % Fe) is a typical soft magnetic material with fcc structure. Recently, single-crystal soft magnetic thin films are used in advanced magnetic devices such as tunneling magnetoresistance sensors and magnetic random access memories, where the films are often exposed to alternating magnetic fields. Magnetostriction behavior of soft magnetic film gives an influence on the performance of such device. Magnetostriction has been measured for epitaxial, polycrystalline, and amorphous magnetic films [1]–[5]. However, there are few studies of magnetostriction focussing on the crystallographic orientation of single-crystal film, though magnetostriction behavior is known to depend on the crystallographic orientation of magnetic material. In the present study, Py epitaxial thin films with three kinds of orientation, fcc(111), fcc(100), and fcc(110), are prepared on single-crystal substrates. A polycrystalline Py film is also prepared. The effect of crystallographic property on the magnetostriction behavior under rotating magnetic fields is investigated for these Py thin films.

2 Experimental procedure

A radio-frequency (RF) magnetron sputtering system equipped with a reflection high-energy electron diffraction (RHEED) facility was used for film preparation. The base pressures were lower than 4×10^{-7} Pa. Py (Ni - 20 at. % Fe), Co, Cu, Pd, and Ag targets of 3 in. diameter were employed. The distance between target and substrate was fixed at 150 mm and the Ar gas pressure was kept constant at 0.67 Pa. The RF powers for Py, Co, Cu, Pd, and Ag targets were respectively adjusted to be 50, 49, 29, 30, and 23 W, where the deposition rate was 0.02 nm/s for all materials.

Py epitaxial films with three kinds of orientation and a polycrystalline film were prepared by using single-crystal substrates (Al_2O_3(0001), MgO(100), and GaAs(110)) and a Si substrate with natural oxide layer, respectively. The film layer structures were Py(500)/Co(5)/Al_2O_3, Py(500)/Cu(10)/Pd(5)/MgO, Py(500)/Cu(20)/Ag(10)/GaAs, and Py(500)/Si, where the values in parenthesis are film thicknesses in nanometers. The thickness of Py film was fixed at 500 nm, while those of Al_2O_3, MgO, GaAs, and Si substrates were respectively 420, 500, 372, and 400 μm. In order to prepare Py epitaxial films of (111), (100), and (110) orientations, Co(0001), Cu(100), and Cu(110) single-crystal underlayers were prepared through hetero-epitaxial growth on Al_2O_3(0001), MgO(100), and GaAs(110) substrates, respectively. The details of underlayer formation are reported in our previous studies [6, 7]. Py epitaxial and polycrystalline films were deposited at a substrate temperature of 300 °C. There is a possibility that atomic diffusion occurs around the Py/Cu interface, since the elevated substrate temperature was used. However, the influence of Cu diffusion on the magnetic property is considered very small, since the Py film thickness is far larger than that of Cu underlayer.
The surface structure was studied by RHEED. The structural properties were investigated by θ-2θ scan X-ray diffraction (XRD) with Cu-Kα radiation (wave length: 0.15418 nm). The magnetization curves were measured by using a vibrating sample magnetometer. The magnetization structure was observed by Bitter method.

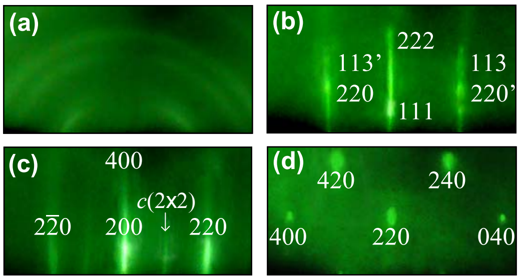

Fig. 1. RHEED patterns observed for (a) a Py film deposited on Si substrate and (b)–(d) Py films grown on (b) Co(0001), (c) Cu(100), and (d) Cu(110) single-crystal underlayers. The incident electron beam is parallel to (b) Co[$11\bar{2}0$] or (c, d) Cu[001].

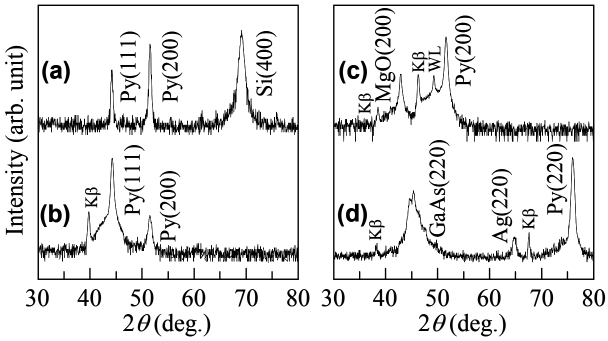

Fig. 2. XRD spectra of (a) Py/Si, (b) Py/Co/Al_2O_3(0001), (c) Py/Cu/Pd/MgO(100), and (d) Py/Cu/Ag/GaAs(110) specimens. The intensity is shown in a logarithmic scale.

The magnetostriction was measured by cantilever method using a laser displacement meter under rotating magnetic fields up to 1000 Oe [8]. The rotating field is applied in in-plane. The saturation magnetostriction, λ_s, was calculated by the following relation,

$$\lambda_s = \frac{\Delta S \times t_s^2}{3 \times L^2 \times t_f} \times \frac{E_s \times (1 + \nu_f)}{E_f \times (1 - \nu_s)}, \tag{1}$$

where ΔS is the measured bending (2nd harmonic output value of magnetostriction), L is the distance between laser beam points, t is the thickness, E is Young's modulus, ν is Poisson's ratio, and the subscripts of f and s respectively refer to film and substrate. The ΔS was estimated when the film was magnetically saturated under rotating magnetic fields, that is, when the 2nd harmonic output showed a constant value. Magnetostriction coefficients of λ_{100} and λ_{111}, were estimated by a formula [9],

$$\begin{aligned}\lambda_s = &\frac{3}{2}\lambda_{100}\left(\alpha_1^2\beta_1^2+\alpha_2^2\beta_2^2+\alpha_3^2\beta_3^2-\frac{1}{3}\right)\\ &+ 3\lambda_{111}(\alpha_1\alpha_2\beta\beta_2+\alpha_2\alpha_3\beta_2\beta_3+\alpha_3\alpha_1\beta_3\beta_1),\end{aligned} \tag{2}$$

where the α is the cosine of the angle between the magnetization and the three crystal axes and the β is the cosine of the angle between the direction of the relative change in length and the crystal axes.

3 Results and discussion

Figures 1(a) and 2(a) show the RHEED pattern and the XRD spectrum of a Py film deposited on Si substrate, respectively. A ring RHEED reflection typical for polycrystalline structure is observed. Py(111) and Py(200) XRD reflections are recognized. A polycrystalline Py film is formed. Figure 1(b) shows the RHEED pattern and the spot map of a Py film grown on Co(0001) underlayer. A clear diffraction pattern corresponding to fcc(111) texture is recognized. The pattern is analyzed to be an overlap of two fcc(111) reflections, as shown by the indices with and without prime. The epitaxial orientation relationships are determined by RHEED as Py(111)[$1\bar{1}0$], (111)[$\bar{1}10$] || Co(0001)[$11\bar{2}0$]. A Py epitaxial film consisting of two fcc(111) variants, whose atomic stacking sequences of close-packed plane along the perpendicular direction are ABCABC… and ACBACB…, is formed on the Co single-crystal underlayer. Figure 2(b) shows the XRD spectrum of Py film formed on Co(0001) underlayer. Py(111) reflections are clearly observed. A weak Py(200) reflection is also recognized, though the RHEED reflection from fcc(100) crystal is not detected. This result suggests that the Py film involves a small volume of fcc(100) crystal. The volume ratio of Py(111) to Py(100) crystal is estimated by XRD [10] to be 98:2. Figures 1(c) and (d) show the RHEED patterns of Py films grown on Cu(100) and Cu(110) underlayers, respectively. Clear RHEED reflections corresponding to fcc(100) and fcc(110) single-crystal surfaces are respectively observed for the films grown on Cu(100) and Cu(110) underlayers, as shown by the indices in RHEED patterns. The epitaxial orientation relationships of Py(100)[001] || Cu(100)[001] and Py(110)[001] || Cu(110)[001] are determined. Single-crystal Py films of (100) and (110) orientations are obtained. Py(200) and Py(220) XRD reflections are respectively observed for the Py films grown on Cu(100) and Cu(110) underlayers, as shown in figures 2(c) and (d).

Figures 3(a) and (b) show the magnetization curves measured for Py polycrystalline and Py(111) epitaxial films, respectively. The hysteresis loops are almost isotropic in the in-plane measurements not only for the polycrystalline film but also for the (111)-oriented epitaxial film. The reason is attributable to the complicated easy magnetization axis distribution in the Py(111) film. The Py(111) film consists of two fcc(111) variants whose orientations are rotated around the film normal by 180° each other and the easy magnetization axes are parallel to [$1\bar{1}1$], [$11\bar{1}$], and [$\bar{1}11$] which are 20° canted from the in-plane and the angle between these orientations is 120°. Figure 3(c) shows the magnetization curves of Py(100) single-crystal film. The film is easily magnetized when the magnetic field is applied along [011], whereas the hysteresis loop measured along [001] saturates at a higher field. The in-plane magnetization property is considered to be reflecting the magnetocrystalline anisotropy of bulk Py crystal and the demagnetization field, since the four easy magnetization axes parallel to <111> directions are 35° inclined from the substrate surface. Figure 3(d) shows the magnetization curves of Py(110) single-crystal film. The film shows a weak uniaxial magnetic anisotropy. The easy magnetization direction is observed along [001], whereas the hard direction is recognized along [$1\bar{1}0$]. The result is in agreement with a theoretical study showing the in-plane easy magnetization direction of fcc(110) single-crystal films with negative 1st magnetocrystalline anisotropy constants [11].

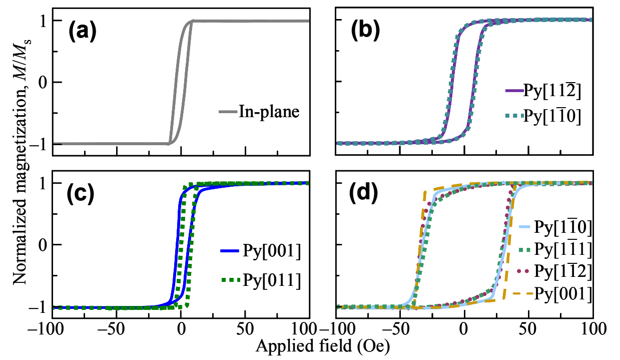

Fig. 3. Magnetization curves measured for (a) a Py polycrystalline film and (b)–(d) Py epitaxial films of (b) (111), (c) (100), and (d) (110) orientations.

Figures 4 and 5 show the output waveforms and the 2nd harmonic outputs of magnetostriction measured for the Py polycrystalline and the Py(111) epitaxial films, respectively. Magnetic fields are applied by varying the angle from 0° to 360°, where the rotation angle is measured between the magnetic field direction and Py[$\bar{1}$10] or Py[1$\bar{1}$0] for the Py(111) film. Usual sinusoidal waveforms are observed under rotating fields ranging from 10 to 1000 Oe. For both films, the 2nd harmonic output increases with increasing the magnetic field up to 20 Oe and the output is kept constant beyond the field, where these films are magnetically saturated. The ΔS of polycrystalline and (111)-oriented films are estimated to be 0.0307 and 0.0067, and the λ_s are thus calculated to be 6×10^{-6} and 5×10^{-6}, respectively. There is a possibility that the λ_s of (111)-oriented film involves a small error, since the film includes a small amount of fcc(100) crystal. In the case of (111)-oriented film, the direction of magnetostriction measurement is along fcc[1$\bar{1}$0]. The α and β are thus given by $\alpha_1 = (1/\sqrt{2})\cos\psi + (1/\sqrt{6})\sin\psi$, $\alpha_2 = (-1/\sqrt{2})\cos\psi + (1/\sqrt{6})\sin\psi$, $\alpha_3 = \cos\psi$, $\beta_1 = 1$, $\beta_2 = 1$, $\beta_3 = 0$, where ψ is the angle of magnetization direction with respect to [1$\bar{1}$0]. By substituting these values into the equation (2), the λ_s is given as $\lambda_s = \lambda_{100} - (3/2)\lambda_{111}$. However it is not possible to estimate the λ_{100} and the λ_{111} values for the (111)-oriented Py film.

Figures 6(a)–(e) show the output waveforms measured for the Py(100) single-crystal film as a function of rotation angle, where the angle is measured between the magnetic field direction and Py[001]. A triangle waveform is observed under a magnetic field of 10 Oe [figure 6(a)]. Peak values of triangle wave appear when the magnetic field is applied along [001], [010], [00$\bar{1}$], or [0$\bar{1}$0]. These are the hard magnetization directions, as shown by the magnetization curve measurement. The triangle waveform changes with increasing the field beyond 30 Oe [figures 6(b, c)] and the film shows sinusoidal waveforms under rotating fields higher than 100 Oe [figures 6(d, e)], where the magnetization is saturated and the λ_s is calculated to be 4×10^{-6}. In the case of (100)-oriented film, the direction of magnetostriction measurement is along fcc[100]. The α and β are thus given by $\alpha_1 = \cos\theta$, $\alpha_2 = \sin\theta$, $\alpha_3 = 0$, $\beta_1 = 1$, $\beta_2 = 0$, $\beta_3 = 0$, where ψ is the angle of magnetization direction with respect to [001]. By substituting these values into the equation (2), the λ_s is expressed as $\lambda_{100} = (2/3)\lambda_s$. The λ_{100} is thus calculated to be 3×10^{-6}. The triangle magnetostriction behavior is possibly related with the magnetic domain wall motion in the magnetically unsaturated film. Figure 7 shows the Bitter image observed for the Py(100) film. 180° magnetic domain walls are apparently formed along the Py[011] direction, which is reflecting the in-plane magnetic anisotropy of Py material. The relation between triangular waveform and magnetic domain wall motion is discussed in the reference [12]. The magnetostriction phenomenon observed in the present study is considered to be influenced by the 180° magnetic domain wall motion under a rotating magnetic field.

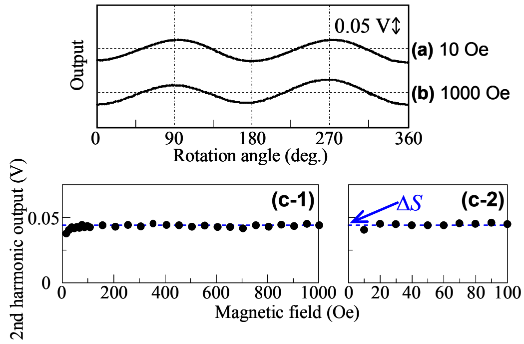

Fig. 4. (a, b) Output waveforms of magnetostriction of a Py polycrystalline measured under magnetic fields of (a) 10 and (b) 1000 Oe. (c-1, c-2) 2nd harmonic output of magnetostriction as a function of applied magnetic field.

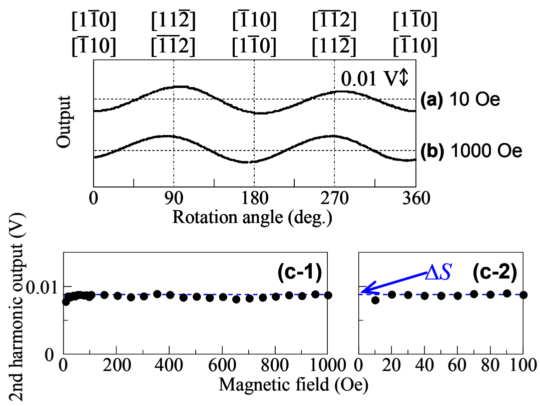

Fig. 5. (a, b) Output waveforms of magnetostriction of a Py(111) epitaxial film measured under magnetic fields of (a) 10 and (b) 1000 Oe. (c-1, c-2) 2nd harmonic output of magnetostriction as a function of applied magnetic field.

Figures 8(a)–(e) show the output waveforms measured for the Py(110) single-crystal film, where the rotation angle is measured from Py[001]. A waveform consisting of a mixture of sinusoidal and triangular shapes is observed under a magnetic field of 10 Oe [figure 8(a)]. Such waveform is very similar to that observed for oriented silicon steel plate [13]. A sinusoidal shape is observed when the field is rotated from [1$\bar{1}\bar{1}$] to [$\bar{1}$1$\bar{1}$] and from [$\bar{1}$11] to [1$\bar{1}$1] (i.e. easy magnetization directions), whereas that of triangle is recognized when the field is rotated from [1$\bar{1}$1] to [1$\bar{1}\bar{1}$] and from [$\bar{1}$1$\bar{1}$] to [$\bar{1}$11] (i.e. hard magnetization directions). When the field is applied along the hard magnetization direction, the film is not magnetically saturated and domain walls reflecting the in-plane magnetic anisotropy are expected to be formed. The magnetostriction behavior of Py(110) single-crystal film is also considered to be influenced by the

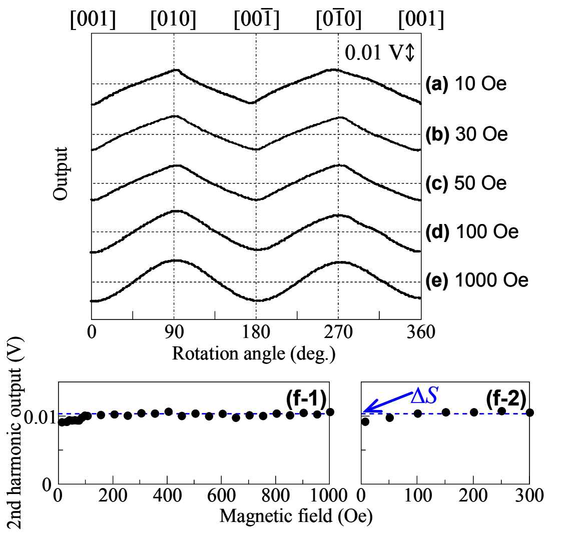

Fig. 6. (a)–(e) Output waveforms of magnetostriction of a Py(100) single-crystal film measured under magnetic fields of (a) 10, (b) 30, (c) 50, (d) 100, and (e) 1000 Oe. (f-1, f-2) 2nd harmonic output of magnetostriction as a function of applied magnetic field.

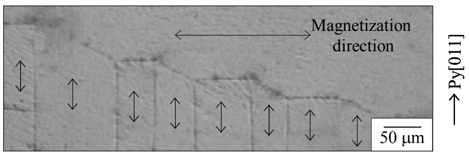

Fig. 7. Bitter image of a Py(100) single-crystal film.

magnetic domain structure. The waveform starts to change with increasing the magnetic field beyond 50 Oe [figures 8(b, c)] and the waveform becomes sinusoidal under magnetic fields higher than 300 Oe [figures 8(d, e)]. Figure 8(f) shows the 2nd harmonic outputs. The output is kept constant at 0.0489 V beyond 300 Oe, where the λ_s value is calculated to be 4×10^{-6}. In the case of (110)-oriented film, the direction of magnetostriction measurement is along fcc[$1\bar{1}0$]. The α and β are thus given by $\alpha_1 = (1/\sqrt{2})\sin\psi$, $\alpha_2 = (1/\sqrt{2})\sin\psi$, $\alpha_3 = \cos\psi$, $\beta_1 = 0$, $\beta_2 = 0$, $\beta_3 = 1$, where ψ is the angle of magnetization direction with respect to [001]. By substituting these values into the equation the (2), the λ_s is expressed as $\lambda_{100} = (2/3)\lambda_s$. The λ_{100} is thus calculated to be 3×10^{-6}. The λ_{100} values estimated for the (100)- and the (110)-oriented films are larger than the bulk Py value ($\lambda_{100} = 2 \times 10^{-6}$). The reason seems to be attributable to the form of sample involving some other factors such as film thickness, shape, film strain or stress, etc.

4 Summary

Py epitaxial films of (111), (100), and (110) orientations and a Py polycrystalline film are prepared. The magnetostriction behavior of theses films are compared. Sinusoidal waveforms are observed, when the magnetostriction is observed as a function of angle between the magnetic field and the sample orientation, under magnetic fields from 10 to 1000 Oe for the (111)-oriented epitaxial and the polycrystalline films. A triangle waveform and a waveform consisting of triangular and sinusoidal shapes are observed for the (100)- and the (110)-oriented single-crystal films, respectively. The

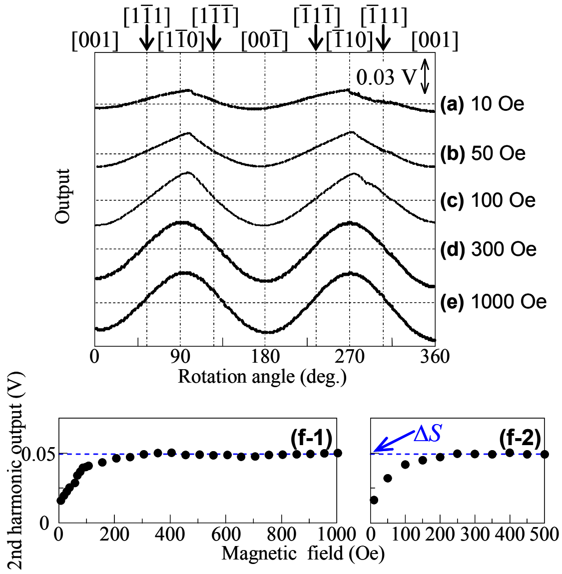

Fig. 8. (a)–(e) Output waveforms of magnetostriction of a Py(110) single-crystal film measured under magnetic fields of (a) 10, (b) 30, (c) 50, (d) 100, and (e) 1000 Oe. (f-1, f-2) 2nd harmonic output of magnetostriction as a function of applied magnetic field.

triangle waveform is related to the motion of magnetic domain walls in magnetically unsaturated film. The triangle waveform changes to a sinusoidal waveform with increasing the magnetic field, where the magnetization is saturated. The λ_s values are determined for the (111)-, the (100)-, the (110)-oriented epitaxial films and the polycrystalline film to be 5×10^{-6}, 4×10^{-6}, 4×10^{-6}, and 6×10^{-6}, respectively.

Acknowledgments

A part of this work was supported by MEXT-Japan.

References

1. D. Markham, N. Smith, IEEE Trans. Magn. **25**, 4198 (1989)
2. R. Bonin *et al.*, J. Appl. Phys. **98**, 123904 (2005)
3. H. Takahashi *et al.*, Jpn. J. Appl. Phys. **32**, L1328 (1993)
4. D. Sander, J. Kirschner, Phys. Status Solidi B **248**, 2398 (2011)
5. Z. Tian *et al.*, Phys. Rev. B **79**, 024432 (2009)
6. M. Ohtake *et al.*, J. Phys.: Conf. Ser. **303**, 012016 (2011)
7. M. Ohtake *et al.*, J. Appl. Phys. **109**, 07C105 (2011)
8. T. Kawai *et al.*, Thin Solid Films **519**, 8429 (2011)
9. B. D. Cullity and C. D Graham, *Introduction to Magnetic Materials* (Addsion-Wesley, Massachusetts, 1972) chap. 8
10. B. D. Cullity, in *Elements of X-Ray Diffraction* (Addsion-Wesley, Massachusetts, 1956) pp. 104–137
11. J. E. Fisher, J. Goddard, J. Phys. Soc. Jpn. **25**, 413 (1968)
12. T. Kawai *et al.*, Abstr. Euromat 2011, p. 2439 (2011)
13. M. Enokizono *et al.*, IEEE Trans. Magn. **26**, 2067 (1990)